State and Spectral Properties of Chloride Oscillations in Pollen

Laura Zonia* and José A. Feijó†
*Institute of Experimental Botany, Academy of Sciences of the Czech Republic, Na Pernikarce 15, 160 00 Prague 6, Czech Republic and †Instituto Gulbenkian Ciência, R. Quinta Grande 6, PT-2780-156 Oeiras, Portugal

ABSTRACT Pollen tube growth is a dynamic system expressing a number of oscillating circuits. Our recent work identified a new circuit, oscillatory efflux of Cl^- anion from the pollen tube apex. Cl^- efflux is the first ion signal found to be coupled in phase with growth oscillations. Functional analyses indicate an active role for Cl^- flux in pollen tube growth. In this report the dynamical properties of Cl^- efflux are examined. Phase space analysis demonstrates that the system trajectory converges on a limit cycle. Fourier analysis reveals that two harmonic frequencies characterize normal growth. Cl^- efflux is inhibited by the channel blocker DIDS, is stimulated by hypoosmotic treatment, and is antagonized by the signal encoded in inositol 3,4,5,6-tetra*kis*phosphate. These perturbations induce transitions of the limit cycle to new metastable states or cause system collapse to a static attractor centered near the origin. These perturbations also transform the spectral profile, inducing subharmonic frequencies, transitions to period doubling and tripling, superharmonic resonance, and chaos. These results indicate that Cl^- signals in pollen tubes display features that are characteristic of active oscillators that carry frequency-encoded information. A reaction network of the Cl^- oscillator coupled to two nonlinear feedback circuits that may drive pollen tube growth oscillations is considered.

INTRODUCTION

Reproductive success in flowering plants depends on bringing the nonmotile sperm cells into contact with egg cells that are deeply embedded inside multiple layers of tissues within the flower. The vehicle that has evolved to accomplish this function is pollen. Mature pollen is dehydrated and metabolically quiescent; after release from the plant it must survive in a free state for an indeterminate period of time. Upon landing on a receptive stigmatic surface it must rapidly hydrate, become biochemically active, and germinate. Growth at the apex is polarized and manifests as the pollen tube, a long cylindrical projection of the cell that penetrates the outer papillar cell layer and grows through the style to ultimately arrive at the entrance to the embryo sac. Once in contact with these specialized cells, the apical region of the pollen tube undergoes a rapid and lethal increase in cell volume that causes the cell to explode near the apex. The force of the explosion propels the sperm cells into the embryo sac to affect fertilization (Mascarenhas, 1993; Taylor and Hepler, 1997; Higashiyama et al., 2000; Feijó et al., 2001; Hepler et al., 2001).

Pollen cell biology is uniquely adapted to these complex conditions. The pollen tube is an emergent system in which order is rapidly achieved by dynamic circuits that enable optimum growth and function under variable extracellular conditions. Pollen tube growth exhibits bistability and can occur with stochastic processes during steady-state growth or with quasisinusoidal oscillatory dynamics. This observation has impelled numerous studies to identify signals that regulate growth oscillations. Oscillatory growth is correlated with oscillatory influx of Ca^{2+}, H^+, and K^+ at the pollen tube apex (Pierson et al., 1996; Holdaway-Clarke et al., 1997; Messerli and Robinson, 1998; Feijó et al., 1999; Messerli et al., 1999), and with oscillations in the tip-localized free Ca^{2+} gradient (Pierson et al., 1994; Messerli et al., 2000). Dissipation of the intracellular free Ca^{2+} gradient or disruption of influx of extracellular Ca^{2+} inhibits pollen tube growth, demonstrating that Ca^{2+} ion dynamics are necessary for pollen tube growth (Pierson et al., 1994). However, correlation analyses revealed that these cation circuits are differentially phase-delayed with respect to growth oscillations (Holdaway-Clarke et al., 1997; Feijó et al., 1999; Messerli et al., 1999, 2000). These observed phase shifts indicate that the start of Ca^{2+}, H^+, and K^+ cycles do not directly correlate with the start of growth cycles, and so these circuits may be passive oscillators coupled to a wider reaction network driving pollen tube growth oscillations.

Using the noninvasive self-referencing ion-specific vibrating electrode probe technology to measure current near the cell surface, our recent work identified a new dynamic circuit that involves oscillatory efflux of Cl^- anion from the pollen tube apex (Zonia et al., 2001, 2002). Oscillatory Cl^- efflux is the first ion signal found to be temporally coupled in phase with growth oscillations. Cell elongation during the growth pulse occurs during the subphase of the cycle with maximally increasing Cl^- efflux from the apex. Cl^- flux is necessary for pollen tube growth and is correlated with the cell volume or hydrostatic condition of the apical region, in that Cl^- channel blockers inhibit pollen tube growth and induce cell volume increases. At 80 μM DIDS, there is a 59% increase in cell volume and 94% of pollen tubes burst near the apex within 10 min. The apical cell volume of growing pollen tubes is exquisitely sensitive to changes in the

Submitted July 14, 2002, and accepted for publication September 27, 2002.

Address reprint requests to Laura Zonia, Institute of Experimental Botany, Academy of Sciences of the Czech Republic, Na Pernikarce 15, 160 00 Prague 6, Czech Republic. Tel.: +420-2-24310710; Fax: +420-2-33339412; E-mail: zonia@ueb.cas.cz.

0006-3495/03/02/1387/12 $2.00

extracellular osmotic potential and hypoosmotic treatment stimulates Cl^- efflux. In vertebrate cells, Cl^- channels are known to be important regulators of secretory activity, osmoregulation, and membrane electrochemical potential (Chen et al., 1996; Renstrom et al., 2002). Extensive work has demonstrated that Ca^{2+}-activated Cl^- efflux channels are negatively regulated by inositol 3,4,5,6-tetra*kis*phosphate [Ins(3,4,5,6)P_4] (Vajanaphanich et al., 1994; Ismailov et al., 1996; Barrett et al., 1998; Nilius et al., 1998; Xie et al., 1998; Yang et al., 1999; Carew et al., 2000; Ho et al., 2000, 2001; Renstrom et al., 2002). Ins(3,4,5,6)P_4 has been identified in the aquatic plant *Spirodela* (Brearley and Hanke, 1996), and Ins(3,4,5,6)P_4 1-kinase and 4- and 6-phosphatase activities have been detected in *Commelina* mesophyll cells (Brearley and Hanke, 2000). In pollen tubes, Ins(3,4,5,6)P_4 acts in regulatory circuits that target growth, apical cell volume, and Cl^- efflux oscillations. The mean growth rate after treatment with Ins(3,4,5,6)P_4 was decreased by 85%, the apical cell volume increased by 54%, and normal Cl^- efflux was disrupted. These effects were not mimicked by Ins(1,3,4,5)P_4 or Ins(1,3,4,5,6)P_5. In summary, Cl^- flux was found to be an important component of regulatory circuits that control pollen tube homeostasis and polarized growth.

To fully understand the mechanics of pollen tube growth that enable sexual fertilization in higher plants, it will be essential to understand the dynamics of individual circuits within the system. The observation that Cl^- efflux oscillations are coupled in phase with growth oscillations and with the physical processes driving cell elongation stimulated the investigations in this report to analyze the state and spectral properties of Cl^- oscillations in pollen tube growth. The approach taken is an application of the tools of nonlinear dynamics and signal processing to characterize the behavior and solutions of Cl^- oscillations in growing pollen tubes. These methods are particularly useful for this study because they characterize the system dynamics utilizing experimentally derived parameter values, which can then be used to formulate testable models. The results of these analyses suggest that Cl^- signals display features that are characteristic of active oscillators that carry frequency-encoded information. In light of its direct correlation with growth oscillations, its role in hydrostatic regulation, and its potential link to inositol polyphosphate signaling cascades via Ins(3,4,5,6)P_4, the Cl^- oscillator may have a central role in the network of regulatory circuits that drive pollen tube growth.

MATERIALS AND METHODS

Pollen culture

Tobacco (*Nicotiana tabacum*) pollen was germinated as follows. The appropriate mass of pollen to give a final culture density of 0.06 mg ml^{-1} was dispersed in germination medium in plastic petri dishes. Germination medium consisted of 6% sucrose, 1.6 mM H_3BO_3, 200 μM $CaCl_2$, 25 μM MES pH 5.5. Cultures were placed on a rotary shaker at 100 rpm and were allowed to germinate and grow at 23°C for 3–7 h before starting the experiments. Under the culture conditions used, >80% of the pollen tubes had oscillatory growth.

Extracellular chloride flux measurements

A self-referencing ion-selective vibrating electrode probe was used to measure extracellular Cl^- flux near the surface of pollen tubes. The vibrating electrode system was attached to a Nikon Eclipse TE-300 inverted microscope (Tokyo, Japan) that was housed inside a copper sheet Faraday cage. A 20× or 40× PlanApo objective under differential interference contrast was used. Microelectrodes were pulled from 1.5 mm borosilicate glass capillaries (World Precision Instruments, Sarasota, FL) with a Sutter P-98 Flaming Brown electrode puller (Sutter Instruments, Novato, CA), baked at 250°C for 8–12 h, and then vaporized with dimethyl-dichlorosilane (Sigma, St. Louis, MO) for 30 min. The capillaries were backfilled with a 15–20 μm column of 100 mM KCl, then front-loaded with a 20–25 μm column of Cl^--selective liquid exchange cocktail (Fluka, Catalog nr. 24889, Milwaukee, WI). An Ag/AgCl wire electrode holder (World Precision Instruments) was inserted into the back of the electrode and established electrical contact with the bathing solution. A dry reference electrode (World Precision Instruments) was inserted into the sample bath. Signals were measured with a purpose built electrometer (Applicable Electronics, Forestdale, MA). Electrode vibration and positioning were achieved with a stepper-motor-driven three-dimensional positioner. The vibrating electrode oscillates with an excursion distance of 10 μm. A typical cycle was completed in 2.33 s; each cycle includes an adjustable settling time after each move, one measuring period at each end position of the cycle, and the excursion time. The measurement taken nearest to the cell is then subtracted by the measurement taken at the opposite end of the cycle; this represents the self-referencing correction. Cl^- flux was measured by vibrating the electrode tip within 5 μm of the cell surface. Background reference values were subtracted from the μV differential recordings during data processing using Microsoft Excel. Background values of Cl^- in the germination medium during the course of experiments were on the order of Cl^- concentrations measured in pollen tubes using the Microquant assay kit (Merck, Darmstadt, Germany), which indicates that pollen contains a sink of Cl^- ion. Data acquisition, preliminary processing, control of the 3D electrode positioner, and stepper-motor controlled fine focus of the microscope stage were performed with ASET software (Science Wares, East Falmouth, MA and Applicable Electronics). Two separate measurements that are collected for each data point in space include a local voltage in mV and the μV differential in the direction of the flux. The μV differential value measured is negative because of the negative charge on Cl^- anion. The ionic flux at each data point in space is calculated with the formula:

$$J_{(x,y,z)} = D(dC_x/dr),$$

where D = diffusion coefficient (for Cl^-, $D = 2.032 \times 10^{-5}$ cm^2 s^{-1}), dC = concentration differential, and dr = spatial differential (for Cl^-, dr = 10 μm). The value for the concentration differential dC requires further calculation. A given point is defined as an origin of measurement (x,y,z) = (0,0,0) and the next measurement is defined as the differential voltage potential along the direction of electrode vibration (dx,0,0). By utilizing the local voltage in mV, the μV differential recording, an experimentally determined ion concentration calibration equation that gives the Nernst slope (*NS*) and intercept (*NI*), and the efficiency (*eff*) of electrode measurement, dC can be calculated as:

$$\begin{aligned} dC_x &= C(dx,0,0) - C(0,0,0) \\ &= 10\exp[((mV[0,0,0] - \mu V/1000 \times eff) - NI)/NS] \\ &\quad - 10\exp[(mV[0,0,0] - NI)/NS]. \end{aligned}$$

(Prof. Joe Kunkel, University of Massachusetts Vibrating Probe Facility, http://www.bio.umass.edu/biology/kunkel/probe/uv2flux.html).

State and spectral analysis of chloride signals

For time domain analysis, the Cl^- flux values recorded by ASET software (Science Wares and Applicable Electronics) during vibrating probe experiments were converted to absolute flux values. Phase space diagrams were computed by calculating the derivative of the flux J with respect to time (dJ/dt) and plotting against the flux value J. Calculations and plots were performed with Microsoft Excel.

For frequency domain analysis, windowed fast Fourier transforms (FFT) [$f(n)g(n)$] were computed for discrete signals [$f(k)$] of period N (Mallat, 1999):

$$[\mathrm{f}(\mathrm{n}), \mathrm{g}_{\mathrm{m,l}}(\mathrm{n})] = \sum_{\mathrm{n}=0}^{\mathrm{N}-1} \mathrm{f}(\mathrm{n})\, \mathrm{g}(\mathrm{n}-\mathrm{m})\, \exp\left(\frac{-\mathrm{i}2\pi \mathrm{ln}}{\mathrm{N}}\right).$$

This is performed with N FFT procedures of size N. Direct calculation of the discrete Fourier sums is given by

$$\mathrm{f}(\mathrm{k}) = \sum_{\mathrm{n}=0}^{\mathrm{N}-1} \mathrm{f}(\mathrm{n}) \exp\left(\frac{-\mathrm{i}2\pi\, \mathrm{kn}}{\mathrm{N}}\right), \quad \text{for } 0 \le \mathrm{k} \le \mathrm{N}.$$

The FFT algorithm groups the direct calculations into even [$f_e(n)$] and odd [$f_o(n)$] frequency indexes to reduce the complexity:

$$\mathrm{f_e}(\mathrm{n}) = \mathrm{f}(\mathrm{n}) + \mathrm{f}(\mathrm{n}+\mathrm{N}/2),$$
$$\mathrm{f_o}(\mathrm{n}) = \exp\left(\frac{-\mathrm{i}2\pi\mathrm{n}}{\mathrm{N}}\right)\left(\mathrm{f}(\mathrm{n}) - \mathrm{f}\left(\mathrm{n}+\frac{\mathrm{N}}{2}\right)\right).$$

A Hanning orthonormal local cosine basis window was used:

$$\mathrm{g}(\mathrm{n}) = \cos^2(\pi\, \mathrm{n}).$$

Information of the amplitudes computed by the windowed FFT series can be extracted and plotted as a function of the signal frequency [f] to yield a spectral analysis of the constituents of a complex signal, called a power spectrum [$S(f)$]. The power spectrum is the discrete Fourier transform of the covariance $R(k)$:

$$\mathrm{S}(\mathrm{f}) = \mathrm{R}(\mathrm{k}) = \sum_{\mathrm{n}=0}^{\mathrm{N}-1} \mathrm{R}(\mathrm{n}) \exp\left(\frac{-\mathrm{i}2\mathrm{k}\pi\mathrm{n}}{\mathrm{N}}\right).$$

The power spectrum $S(f)$ is plotted against the frequency (f) in Hz. Power distributions were then determined by plotting $\log_{10}[S(f)]$ versus $\log_{10}[f]$ and computing linear regressions. The slopes of the power distribution linear regressions are reported. Computations and plots for windowed fast Fourier transforms, power spectra, and power distributions were performed using customized transforms programmed in SigmaPlot 7.1 (SPSS Science Inc., Chicago, IL).

Inositol 3,4,5,6-tetra*kis*phosphate studies

Ins(3,4,5,6)P_4 was synthesized by Matreya Inc. (Pleasant Gap, PA) and obtained through BioTrend Chemikalien GmbH (Köln, Germany). The experimental conditions for inositol polyphosphate studies were previously reported in detail (Zonia et al., 2002). Microinjection of Ins(3,4,5,6)P_4 inhibits pollen tube growth by 85% and this effect is not mimicked by either Ins(1,3,4,5)P_4 or Ins(1,3,4,5,6)P_5. Extracellular addition of Ins(3,4,5,6)P_4 inhibits pollen tube growth by 66%, rapidly induces increases of 54% in the pollen tube apical cell volume compared with untreated controls (which is on the order of the mean maximum volume load for cell bursting, which is a 59% volume increase, induced by the Cl^- channel blocker DIDS), and disrupts normal Cl^- efflux oscillations. These effects are not mimicked by either Ins(1,3,4,5)P_4 or Ins(1,3,4,5,6)P_5. For the studies in this report, Ins(3,4,5,6)P_4 was added extracellularly to the pollen tube cultures because the integrity of the Cl^- efflux signal is sensitive to mechanical perturbation. Recent work has identified sites of active membrane turnover in the pollen tube apical region that may provide a route for fluid-phase uptake of inositol polyphosphates into the cytosol (L. Zonia, unpublished). Intracellular concentrations of Ins(3,4,5,6)P_4 in epithelial cells rise from ~1 μM in resting cells to 10–15 μM after cell activation (Pittet et al., 1989; Vajanaphanich et al., 1994). For the studies in this report Ins(3,4,5,6)P_4 was added to the pollen tube cultures at a concentration of 20 μM.

Reagents

DIDS (4,4′-diisothiocyanatostilbene-2,2′-disulfonic acid) was from Sigma. All other chemicals were plant cell culture or reagent grade and were from Sigma or Fluka.

RESULTS

Chloride oscillations converge on a limit cycle and have harmonic frequencies

Cl^- current becomes organized as sustained quasisinusoidal efflux from the apex when tobacco pollen tubes reach lengths >500 μm (Fig. 1 *A*). The amplitudes of Cl^- efflux varied across heterogeneous populations of pollen between values of 400–3000 pmol Cl^- cm^{-2} s^{-1}. The magnitude of Cl^- efflux also varied by one order of magnitude across heterogeneous populations of pollen, with most cycling within boundary values of 1000–10,000 pmol Cl^- cm^{-2} s^{-1}. The dynamics of Cl^- efflux were analyzed in the phase space to examine the long-term behavior of the system. As shown in Fig. 1 *B*, the system converges on a limit cycle. To characterize the frequency domain of these oscillations, power spectral analyses were performed. As shown in Fig. 1 *C*, the dynamics of this pollen tube are resolved in a primary frequency at 0.02 Hz, or period of 50 s, with power 1.5×10^9. The power distribution linear regression slope equals −1.83 (Fig. 1 *C*, *inset*). The frequency resolved at 0.02 Hz appropriately represents the periodicity observed for Cl^- efflux oscillations in the time domain (Fig. 1 *A*). Analyses of Cl^- signals in other tobacco pollen tubes indicate that during normal oscillatory growth the system expresses one or two harmonic frequencies at 0.01 and 0.02 Hz, or periods of 100 s and 50 s, with power of the order 10^8–10^9 ($n = 12$) (see also the following sections). Periods of 100 s and 50 s correlate with the observed periodicity of growth rate oscillations in tobacco pollen tubes as reported previously (Zonia et al., 2002).

The limit cycle collapses to a fixed-point attractor near the origin upon perturbation with a chloride channel blocker

To begin to understand the response dynamics of the system, it was subjected to strong perturbation in the form of the Cl^- channel blocker DIDS ($n = 6$). As shown in Fig. 2 *A*, Cl^- oscillations are severely disrupted after addition of 80 μM DIDS. The limit cycle immediately collapsed to a fixed-point attractor near the origin and within 150 s the pollen tube burst near the apex due to the lethal increase in cell volume caused by DIDS. Power spectral analysis showed that before

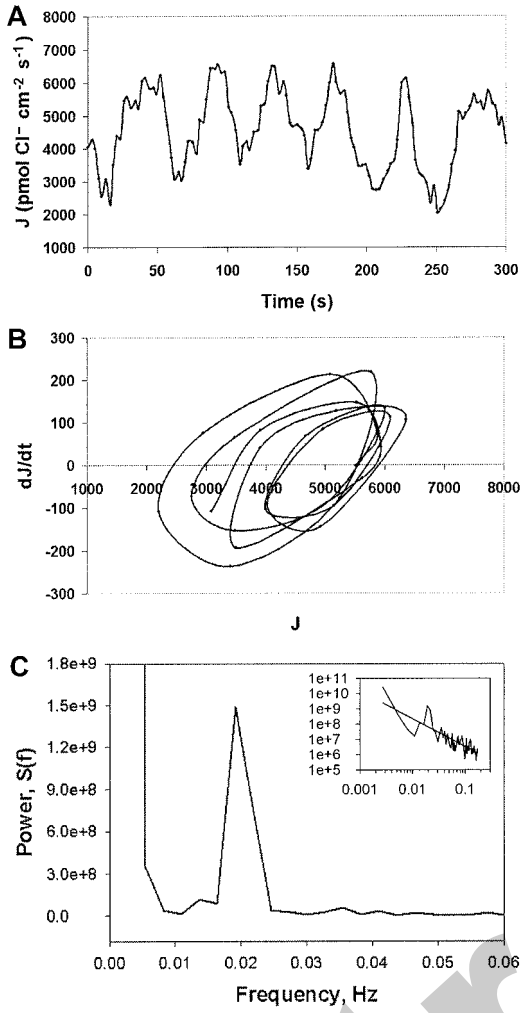

FIGURE 1 State and spectral properties of Cl^- efflux oscillations in tobacco pollen. (*A*) Cl^- flux versus time plot. (*B*) Phase space diagram. (*C*) Power spectral analysis. The inset shows the power distribution, $\log_{10}[S(f)]$ versus $\log_{10}[f]$, and the linear regression.

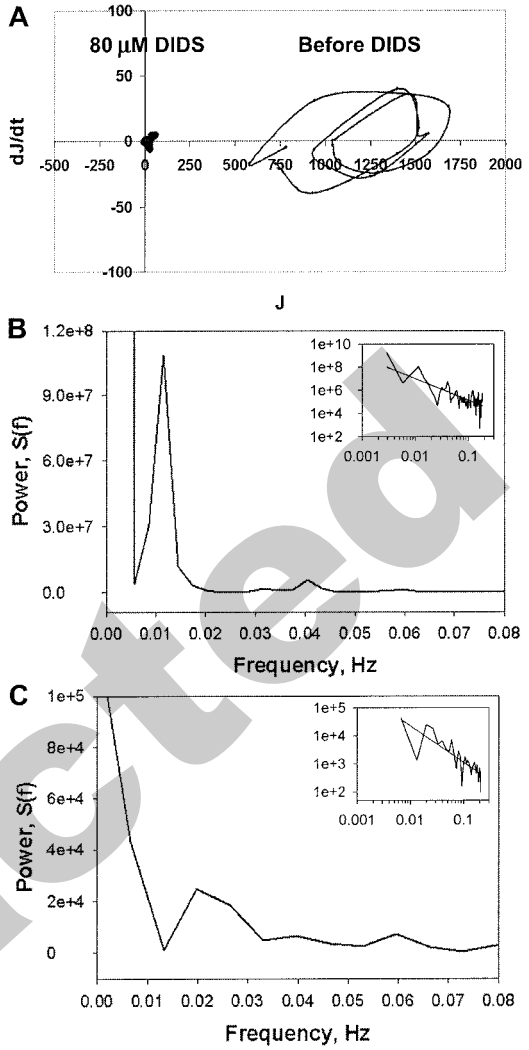

FIGURE 2 Effect of the Cl^- channel blocker DIDS on the state and spectral properties of Cl^- efflux oscillations. (*A*) Phase space diagrams before treatment (●) and after treatment with 80 μM DIDS (●). The pollen tube burst at the apex 150 s after addition of 80 μM DIDS. (*B*) Power spectrum before treatment. (*C*) Power spectrum after addition of 80 μM DIDS. Insets in *B* and *C* show the power distributions, $\log_{10}[S(f)]$ versus $\log_{10}[f]$, and the linear regressions.

treatment the main frequency resolved at 0.01 Hz (100-s period) with power of 1.1×10^8 (Fig. 2 *B*); the power distribution linear regression slope equals -1.88 (Fig. 2 *B*, *inset*). Immediately after treatment with 80 μM DIDS, the 0.01 Hz frequency was abolished and a residual frequency emerges at 0.02 Hz (50-s period) with depleted power of 2.5×10^4 (Fig. 2 *C*); the power distribution linear regression slope equals -1.30 (Fig. 2 *C*, *inset*). These results indicate that the Cl^- signal frequency is rapidly dissipated in response to inhibitor perturbation, and that severe depletion of energy from the system occurs concurrently with the inhibitor-induced processes that cause lethal cell swelling and death.

Hypoosmotic treatment induces transitions of the limit cycle and the chloride frequency

Stimulatory driving of the system was achieved by lowering the extracellular osmotic potential. The response of the system dynamics to increasing hypoosmotic conditions is shown in Fig. 3 ($n = 4$). The state properties of Cl^- efflux before treatment are shown in Fig. 3 *A* (limit cycle on *left*). The power spectrum before treatment resolves in the harmonic frequency at 0.01 Hz (100-s period) with power of 3.2×10^9, and a shoulder at 0.005 Hz (200-s period) (Fig. 3 *C*); the power distribution linear regression slope equals -1.81 (Fig. 3 *C*, *inset*). Low levels of hypoosmotic treatment at 2.5% (v/v) H_2O induce a tangential transition of the limit cycle in the phase space with an increased turbulence in the trajectory (Fig. 3 *A*, limit cycle on *right*). The power spectrum transforms to three frequencies, the two harmonic frequencies at 0.01 and 0.02 Hz (100- and 50-s periods, respectively) and in addition a new subharmonic

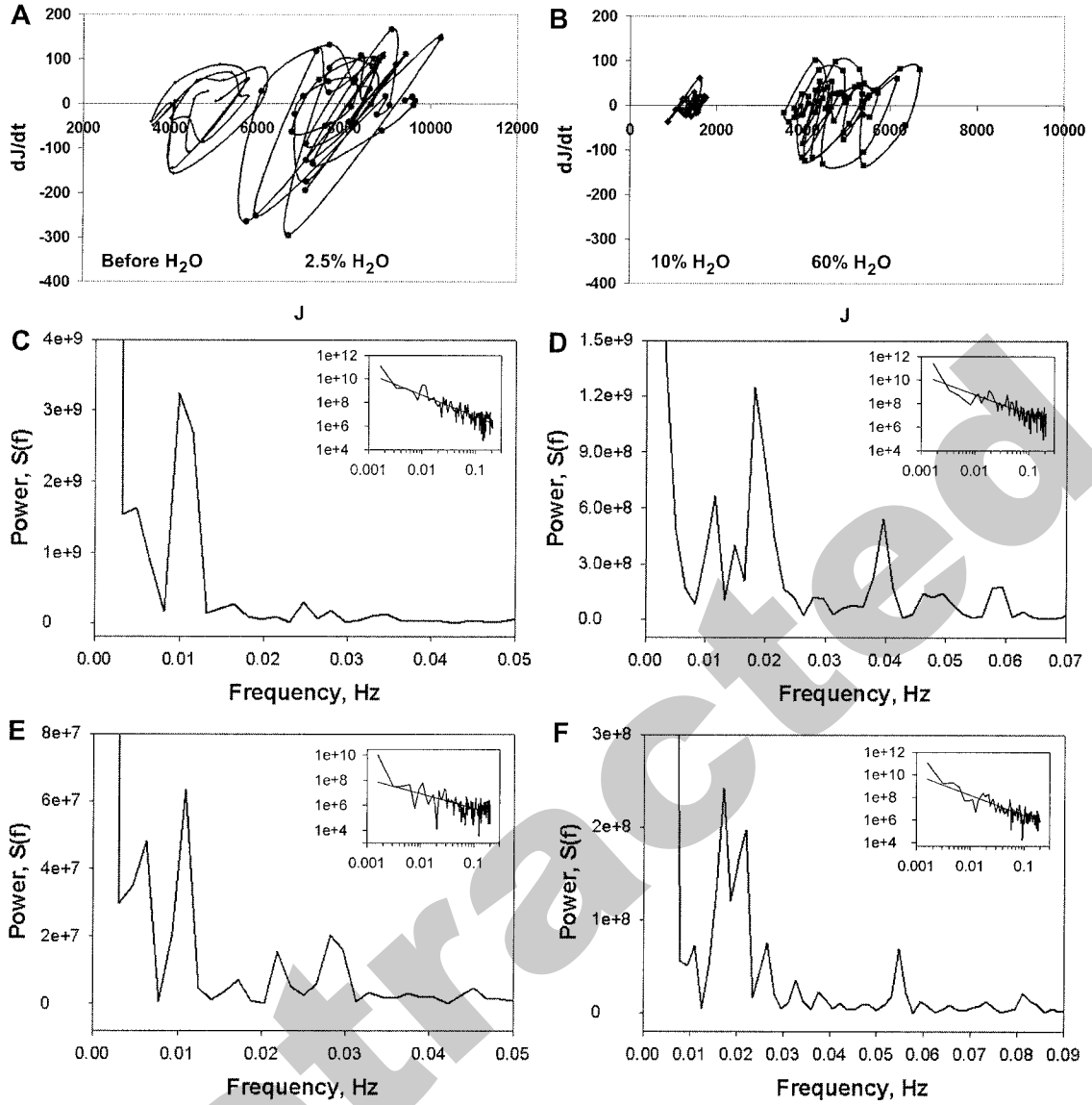

FIGURE 3 Hypoosmotic treatment induces tangential transitions of Cl^- oscillations to new metastable states and modulates the signal frequency. (*A*) Phase space diagrams before treatment (●) and after addition of 2.5% (v/v) H_2O (●). (*B*) Phase space diagrams after addition of 10% (v/v) H_2O (♦) and 60% (v/v) H_2O (■). Note equivalent scaling of the axes in plots *A* and *B*. Power spectra (*C*) before treatment, and after addition of (*D*) 2.5% (v/v) H_2O, (*E*) 10% (v/v) H_2O, and (*F*) 60% (v/v) H_2O. Insets in *C*–F show the power distributions, $\log_{10}[S(f)]$ versus $\log_{10}[f]$, and the linear regressions.

frequency at 0.04 Hz (25-s period) (Fig. 3 *D*); the power distribution linear regression slope equals −1.69 (Fig. 3 *D*, *inset*). With a further increase of hypoosmotic treatment to 10% (v/v) H_2O, there is a dissipation of the system and the attractor moves to more negative regions of the phase space (Fig. 3 *B*, limit cycle on *left*). This response is reflected by transitions in the power spectrum with frequencies at 0.005 and 0.01 Hz (200- and 100-s periods, respectively), and two lower-energy peaks at 0.022 and 0.029 Hz (45- and 34-s periods, respectively), and a depletion of power to the order of 10^7 (Fig. 3 *E*); the power distribution linear regression slope equals −1.15 (Fig. 3 *E*, *inset*). With further hypoosmotic treatment there is an adjustment and restabilization of the system. At the point of 60% (v/v) H_2O, the system has regained stability and the attractor has moved back to the original location in the phase space (Fig. 3 *B*, limit cycle on *right*). The power spectrum reveals that the Cl^- signal frequency has modulated to 0.02 Hz (50-s period), with power of the order 10^8 (Fig. 3 *F*); the power distribution linear regression slope equals −1.79 (Fig. 3 *F*, *inset*). The frequency at 0.005 Hz has essentially returned to the pretreatment state (compare power distributions of Fig. 3, *C* and *F*). The results of these studies indicate that small decreases in the extracellular osmotic potential that have previously been shown to cause cell volume increases stimulate the frequency of Cl^- efflux oscillations (Fig. 3 *D*). A mechanism to adjust to more severe hypoosmotic treatment is suggested by the observation that the limit

cycle returns to the original location in the phase space (Fig. 3, *A* and *B*) and resets the frequency of Cl^- efflux oscillation (Fig. 3, *C* and *F*).

Inositol 3,4,5,6-tetra*kis*phosphate induces transitions to period tripling and chaos

In these studies, Cl^- efflux oscillations for several pollen tubes ($n > 5$) in the same culture were assessed to establish a pattern that was representative of the population. A typical behavior is shown in the phase space diagram in Fig. 4 *A*. Then the Cl^- efflux antagonist Ins(3,4,5,6)P_4 was added (see Methods for details) and the effect on Cl^- efflux was analyzed. In the majority of pollen tubes, the system was severely perturbed ($n = 11$ of a total of 14). The phase space diagrams for four representative examples are shown in Fig. 4, *B–E*. Ins(3,4,5,6)P_4 can cause the system to collapse to a static attractor near the origin ($n = 4$ of the 11) (Fig. 4 *B*). The dynamics for the remaining pollen tubes ($n = 7$ of the 11) was a transition of the attractor to more negative regions of the phase space and an increase in system turbulence (Fig. 4, *C–E*). The power spectrum of the representative pollen tube before treatment shows that both of the harmonic frequencies at 0.01 and 0.02 Hz (100- and 50-s periods, respectively) are present as well as a frequency at 0.006 Hz (167-s period) (Fig. 4 *F*); the power distribution linear regression slope equals −1.59 (Fig. 4 *F*, *inset*). The power spectrum shown in Fig. 4 *G*, which corresponds to the phase space diagram of Fig. 4 *E*, has four frequencies at 0.01, 0.006, 0.0033, and 0.002 Hz (100-, 167-, 303-, and 500-s periods, respectively), with the power distribution linear regression slope equal to −0.67 (Fig. 4 *G*, *inset*). The power spectra shown in Fig. 4, *H* and *I*, which correspond to the phase space diagrams of Fig. 4, *B* and *D*, respectively, have undergone marked transformations. These spectra show the emergence of multiple frequencies across the spectrum and essentially complete dissipation of the 0.01 and 0.02 Hz frequencies, suggesting that the system has transformed to a chaotic state. This is further reflected in the power distribution linear regression slope equal to −0.26 for Fig. 4 *H* (*inset*) and −0.03 for Fig. 4 *I* (*inset*). These results indicate that the signal encoded in Ins(3,4,5,6)P_4 inhibits the frequency of the Cl^- signal, which undergoes transitions to period tripling and multiplicative increases that may provide a route for the emergence of chaos.

Inositol 3,4,5,6-tetra*kis*phosphate can induce resonance states

In the previous section, the response to Ins(3,4,5,6)P_4 manifested by the majority of pollen tubes was presented. The response of the minority of pollen tubes ($n = 3$ out of 14 total) to Ins(3,4,5,6)P_4 is presented in this section. The experiment shown in Fig. 5 is from a recording of Cl^- efflux oscillations in the same pollen tube before and after addition of Ins(3,4,5,6)P_4. The phase space diagram before treatment is turbulent, as shown in Fig. 5 *A*. The power spectrum before treatment shows the two harmonic frequencies at 0.01 and 0.02 Hz (100- and 50-s periods), with power of 2.6×10^8 and 1.3×10^8 respectively, and an unusual frequency at 0.029 Hz (34-s period) (Fig. 5 *C*); the power distribution linear regression slope equals −1.91 (Fig. 5 *C*, *inset*). After addition of Ins(3,4,5,6)P_4 the location of the attractor in the phase space does not significantly change but the system trajectory undergoes a marked transformation and moves out significantly in both dimensions (Fig. 5 *B*). After addition of Ins(3,4,5,6)P_4 the power spectrum resolves in two frequencies at 0.01 and 0.005 Hz (100- and 200-s periods, respectively) (Fig. 5 *D*); the power distribution linear regression slope equals −1.86 (Fig. 5 *D*, *inset*). There is a substantial increase in the system energy: the 0.005 Hz frequency has power of 1.3×10^{10} and the 0.01 Hz frequency has power of 2.5×10^9 (Fig. 5 *D*). These results indicate that the system is undergoing transitions to period doubling with resonance in both the 0.01 Hz harmonic and the 0.005 Hz superharmonic frequencies. This observation of superharmonic resonance suggests that three of 14 pollen tubes undergo a weak damping of Cl^- efflux, likely due to uptake of suboptimal concentrations of Ins(3,4,5,6)P_4, coupled with stimulatory driving of Cl^- efflux by an internal (endogenous) positive feedback circuit.

Examination of steady-state behavior

Pollen tube growth exhibits bistability and can occur without oscillatory dynamics. Steady-state growth displays a relatively steady or randomly fluctuating growth rate and a low and fluctuating level of Cl^- flux at the apex. Phase space diagrams and power spectra were analyzed for pollen tubes under steady-state conditions to assess the properties of Cl^- oscillations during stochastic growth ($n = 5$). The results for two representative examples are shown in Fig. 6. The phase space diagram for the pollen tube in Fig. 6 *A* is converged on a static attractor located near the origin. Nevertheless, the power spectrum reveals a periodic order in the system, with the harmonic frequency at 0.02 Hz (50-s period) and lower-energy noise at higher and lower frequencies (Fig. 6 *C*); the power distribution linear regression slope equals −0.78 (Fig. 6 *C*, *inset*). The turbulent diagram in Fig. 6 *B* is also attracted near the origin but moves out into a local region of the phase space. The power spectrum for this system has the harmonic frequency at 0.01 Hz (100-s period) and lower-energy noise at higher frequencies (Fig. 6 *D*); the power distribution linear regression slope equals −0.68 (Fig. 6 *D*, *inset*). These results indicate that the Cl^- signal harmonic frequencies at 0.01 and 0.02 Hz coexist with random noise in pollen tubes undergoing steady-state growth, which suggests that the Cl^- oscillator may be switched on before the manifestation of quasisinusoidal growth.

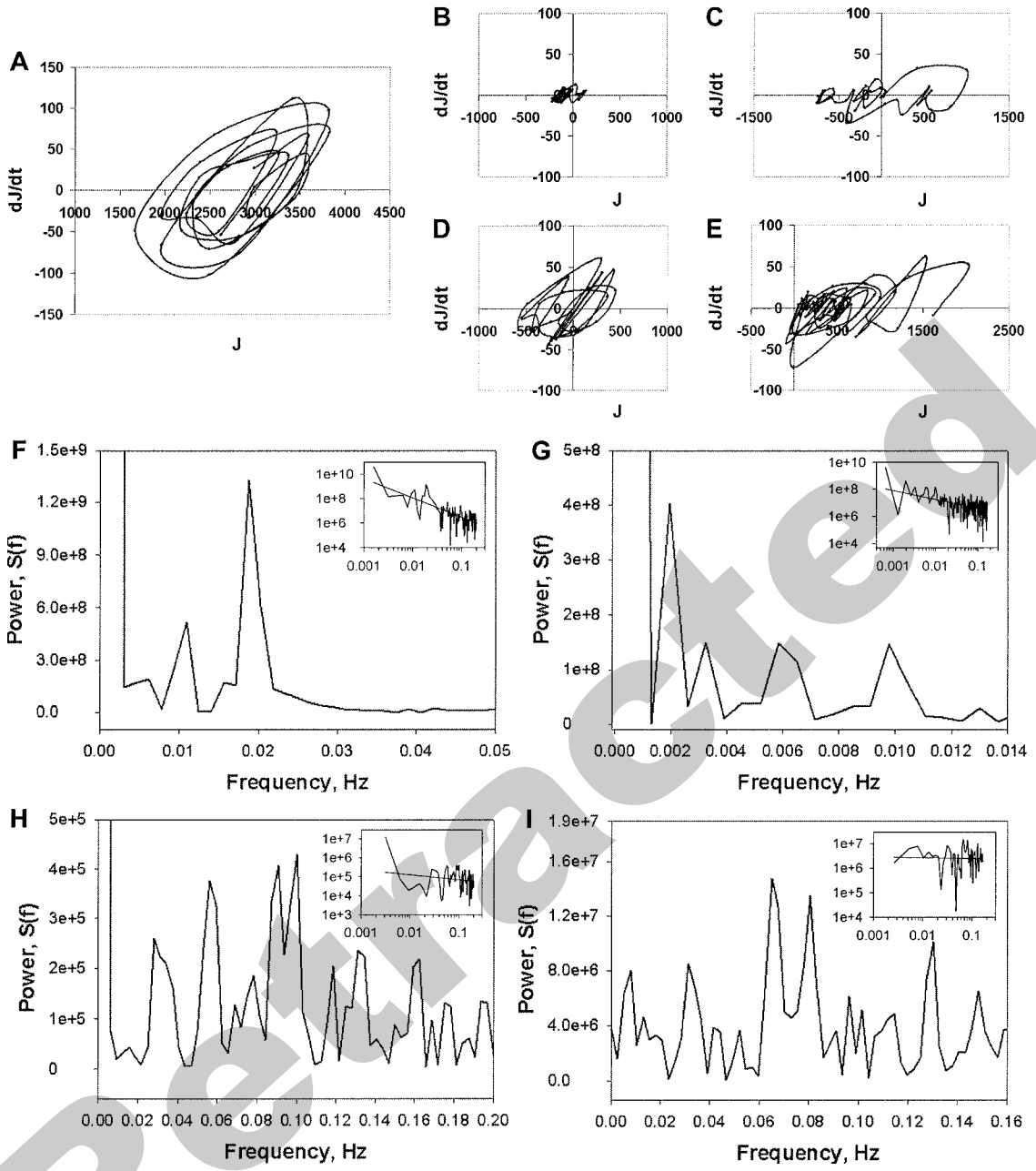

FIGURE 4 Ins(3,4,5,6)P_4 transforms Cl^- dynamics. (*A*) Representative phase space diagram before treatment. (*B–E*) Phase space diagrams of Cl^- dynamics in four different pollen tubes after treatment with 20 μM Ins(3,4,5,6)P_4. Note equivalent scaling of the axes in plots *A–E*. (*F*) Representative power spectrum before treatment; corresponds with the phase space diagram *A*. (*G*) Transitions to period-tripling and higher-order multiplicative states after treatment with Ins(3,4,5,6)P_4; corresponds with the phase space diagram *E*. (*H*) Transformation to chaos after treatment with Ins(3,4,5,6)P_4; corresponds with the phase space diagram *B*. (*I*) Transformation to chaos after treatment with Ins(3,4,5,6)P_4; corresponds with the phase space diagram *D*. Insets in *F–I* show the power distributions, $\log_{10}[S(f)]$ versus $\log_{10}[f]$, and the linear regressions.

DISCUSSION

The significance of nonlinear control in plants

Plant cells are uniquely entrained to extracellular and environmental cues that exhibit periodicity such as light, temperature, and water. Analytical tools of nonlinear dynamics and signal processing have provided important insights into the nonlinear control circuits that organize cellular responses to these periodic cues. Significant progress has been achieved in the analysis of light-dependent responses (Shabala et al., 1997; Rascher et al., 1998; Lüttge, 2000; Bohn et al., 2001; Hafke et al., 2001; Rascher et al., 2001; Bohn et al., 2002) and Ca^{2+} signaling (Allen et al., 2000, 2001). These studies demonstrate that analysis of the

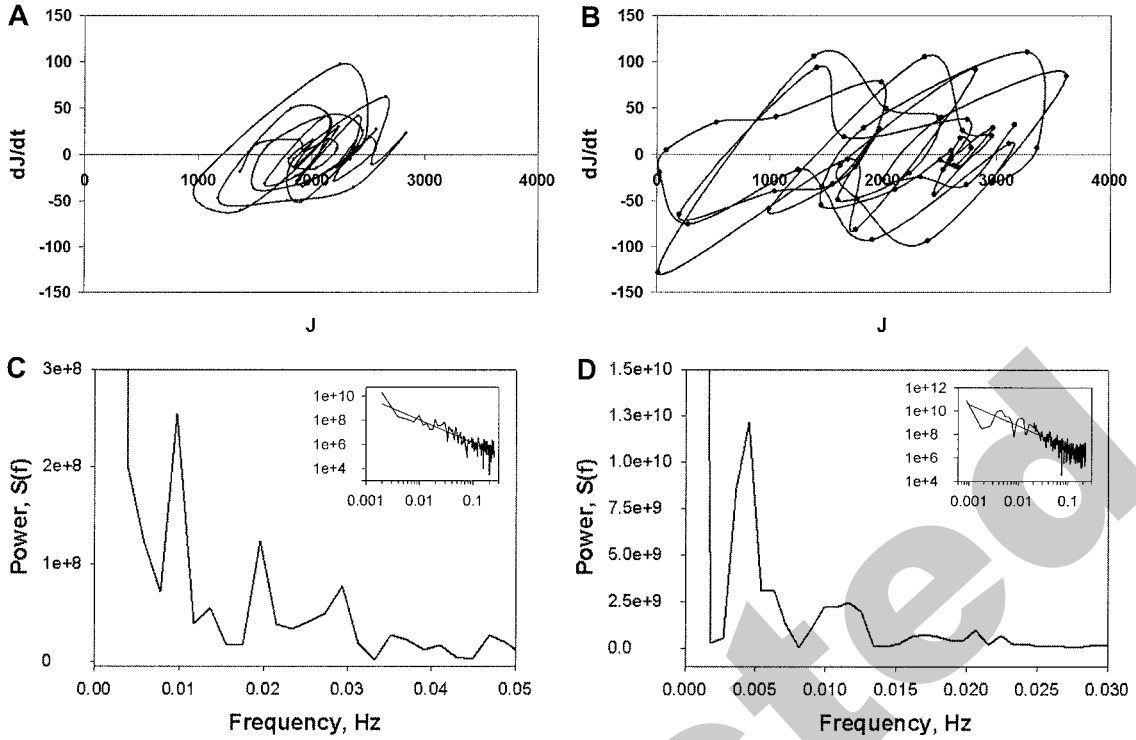

FIGURE 5 Superharmonic resonance induced by Ins(3,4,5,6)P_4. Phase space diagram before (*A*) and after (*B*) treatment with 20 μM Ins(3,4,5,6)P_4. Power spectra before (*C*) and after (*D*) treatment with 20 μM Ins(3,4,5,6)P_4. Note that the $S(f)$ axis scale in *D* is two orders of magnitude greater than in *C*. Insets in *C* and *D* show the power distributions, $\log_{10}[S(f)]$ versus $\log_{10}[f]$, and the linear regressions.

properties that define nonlinear control circuits can reveal important information about mechanisms of cellular signaling in plants.

State and spectral transformations of chloride signals in growing pollen tubes

Cl^- flux is necessary for pollen tube growth and has an important functional role in the processes that mediate cell elongation (Zonia et al., 2002). This report has evaluated Cl^- efflux signals using tools of nonlinear dynamics and signal processing to characterize the properties of the Cl^- oscillator and to further assess the role of Cl^- efflux oscillations during pollen tube growth. The results demonstrate that Cl^- signals exhibit behaviors that are characteristic of active nonlinear harmonic oscillators.

Hypoosmotic treatment induces transitions of the limit cycle to new metastable states and modulates the frequencies of Cl^- efflux oscillations (Fig. 3). Low levels of hypoosmotic treatment have been shown to cause increases in the apical cell volume (Zonia et al., 2002). Treatment with 2.5% (v/v) H_2O stimulates the frequency of Cl^- efflux with periods decreasing from 100 s to 50 s and 25 s (Fig. 3 *D*). Further hypoosmotic treatment of 10% (v/v) H_2O depletes the system energy and causes a transition of the limit cycle to more negative regions of the phase space (Fig. 3, *B* and *E*). This may reflect a transient dissipation of the internal Cl^- pool due to the stimulation of Cl^- efflux and the decreased extracellular osmotic potential. A mechanism to adjust to more severe or prolonged hypoosmotic conditions is suggested by the observation that the system moves back to the original location in the phase space (Fig. 3, *A* and *B*) and the frequency of Cl^- efflux oscillations modulates from the pretreatment period of 100 s to the more rapid period of 50 s (Fig. 3, *C* and *F*). Recent work has indicated that the phospholipid signal phosphatidic acid is induced in pollen tubes during severe hypoosmotic conditions >25–30% (v/v) H_2O (L. Zonia and T. Munnik, unpublished). This result is significant for pollen tubes under severe hypoosmotic stress because activation of the phospholipase D pathway leading to increased phosphatidic acid can potentiate Cl^- efflux during specific programs of cellular activation in vertebrate cells (Vajanaphanich et al., 1993; Oprins et al., 2001, 2002). Taken together, these results indicate that the Cl^- oscillator can progress to new stable states and respond to increases in the intracellular hydrostatic pressure by increasing the frequency of Cl^- efflux.

The Cl^- channel blocker DIDS induces rapid cell volume increases that lead to cell bursting (Zonia et al., 2002). The lethal concentration of 80 μM DIDS causes the system to collapse to a fixed-point attractor near the origin (Fig. 2 *A*). The pollen tube shown in Fig. 2 burst within 150 s after addition of DIDS. Before cell death there was a severe depletion of energy from the system, the frequency at 0.01

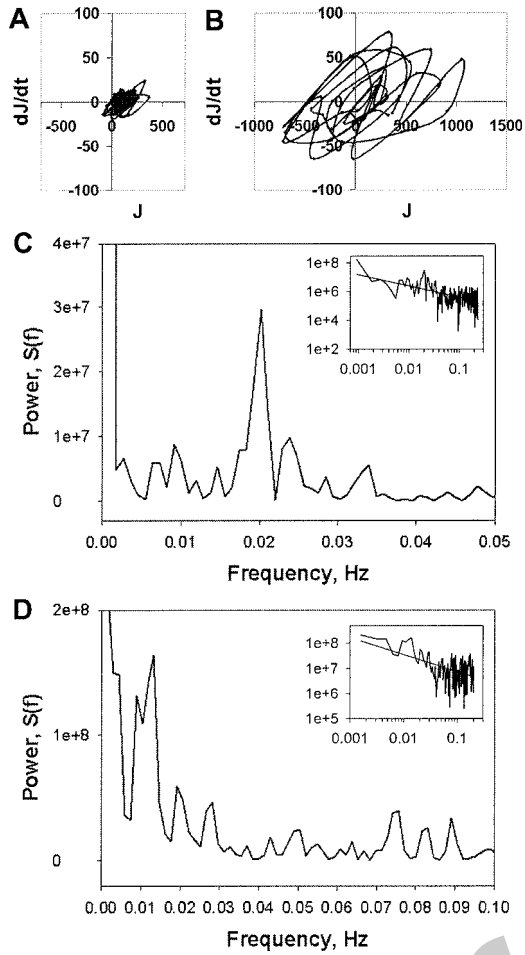

FIGURE 6 Chloride dynamics during stochastic growth of two representative pollen tubes. (*A* and *B*) Phase space diagrams. (*C*) Power spectrum corresponding to the phase space plot *A*. (*D*) Power spectrum corresponding to the phase space plot *B*. Insets in *C* and *D* show the power distributions, $\log_{10}[S(f)]$ versus $\log_{10}[f]$, and the linear regressions.

Hz was obliterated, and a residual frequency emerged at 0.02 Hz (Fig. 2, *B* and *C*). It may be possible that during the rapid increase in intracellular hydrostatic pressure induced by DIDS the Cl^- efflux frequency was driven from 0.01 Hz to 0.02 Hz, a response that was also observed after increases in the intracellular hydrostatic pressure induced by hypoosmotic treatment (Fig. 3).

The signal encoded in Ins(3,4,5,6)P_4 has profound effects on Cl^- efflux oscillations (Fig. 4). In 11 of 14 pollen tubes examined, the system moved to an attractor near the origin with a marked increase of turbulence in the trajectory (Fig. 4, *B–E*). The power spectra indicate that Ins(3,4,5,6)P_4 inhibits the frequency of Cl^- efflux oscillations, with periods increasing from the normal harmonic series of 50 and 100 s (Fig. 4 *F*) to periods of 100–500 s (Fig. 4 *G*). The periods observed (100 s, 167 s, 303 s, 500 s) represent transitions to period-tripling states and states with higher-order multiplicative increases, which may eventually lead to the onset of chaos (Fig. 4, *H* and *I*). In three of 14 pollen tubes examined, superharmonic resonance states were induced after treatment with Ins(3,4,5,6)P_4 (Fig. 5). Superharmonic resonance states in nonlinear oscillators can result from the introduction of weak damping coupled with stimulatory driving of the system (Acheson, 1997). Hence, it is possible that superharmonic resonance is observed in these pollen tubes due to uptake of a suboptimal concentration of Ins(3,4,5,6)P_4 that imperfectly dampens Cl^- efflux oscillations, coupled with stimulatory driving of Cl^- efflux oscillations by an endogenous positive feedback circuit.

The results of these perturbation studies demonstrate that the Cl^- oscillator is poised to rapidly respond to both stimulatory and inhibitory feedback. Positive feedback in the form of increased intracellular hydrostatic pressure drives the system to new states with transient increases in subharmonic signal frequencies (Fig. 3). Negative feedback encoded in Ins(3,4,5,6)P_4 inhibits the frequency of the Cl^- signal, leading to period-tripling and multiplicative increases that may provide a route to chaos (Fig. 4). The results also indicate the existence of an internal positive feedback circuit that can drive Cl^- efflux during weak damping (Fig. 5). In summary, these analyses demonstrate that the Cl^- oscillator has the potential to receive input from both positive and negative feedback circuits that modulate the output frequency of the oscillator. In light of the fact that the Cl^- oscillator is temporally coupled in phase with growth oscillations, and that perturbation of Cl^- efflux also perturbs growth, these results suggest that the Cl^- oscillator may have a central role in driving pollen tube growth.

Hypothesized reaction network regulating chloride oscillations and pollen tube growth

Pollen tube growth is a bistable system that exhibits either stochastic or quasisinusoidal dynamics. Nothing is known of the biophysical factors that determine the switch to oscillatory growth. Signals and cellular factors that are important for the fundamental mechanics of growth should be present irrespective of the system state. The observation that the Cl^- signal harmonic frequencies at 0.01 and 0.02 Hz coexist with a background of noise in pollen tubes undergoing steady-state growth indicates that the Cl^- oscillator signal is a component of the fundamental mechanics that drive growth (Fig. 6). These observations further suggest that the switch from stochastic to oscillatory growth may involve an increase in the biochemical or biomolecular organization of the growing pollen tube. After tobacco pollen tube growth becomes organized into sustained oscillations, the observed periods for normal growth cycle oscillations are identical with the normal harmonic frequencies of the Cl^- oscillator—50 s and 100 s (Zonia et al., 2002).

A minimal reaction network that may be coupled to the Cl^- oscillator during oscillatory growth is shown in Fig. 7.

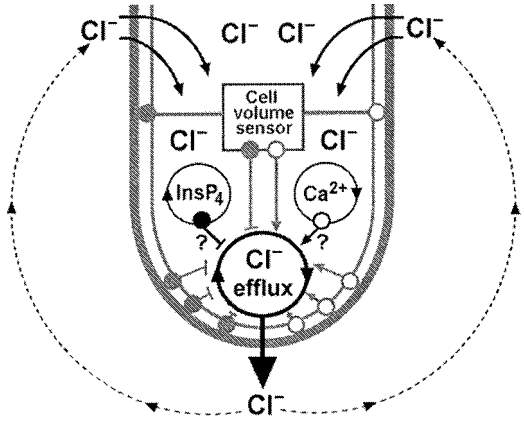

FIGURE 7 Proposed minimal model of Cl^- efflux oscillations in the pollen tube apex. The Cl^- pool at the apex is supplied from Cl^- influx along distal regions of the tube and from an internal sink. Spatial coupling of influx and efflux sites promotes a closed circuit of Cl^- flux surrounding the apical region. Cell volume sensors are denoted by gray nodes and flowlines. The putative Ins(3,4,5,6)P_4 and Ca^{2+} cycles (marked with *?* pending further investigation) are hypothesized to be temporally phase-shifted by 180°. Negative feedback is denoted as ●—I. Positive feedback is denoted as ○→. The thick outline around the cell denotes the cell wall, the thin interior line denotes the plasma membrane. Details are given in the Discussion.

This network includes a sink for Cl^- ions, feedback from cell volume sensors, and input from Ins(3,4,5,6)P_4 and Ca^{2+} as two nonlinear feedback regulators of Cl^- efflux.

Topological mapping of the cell surface identified sites of steady influx of Cl^- along the flanks of the pollen tube in regions adjacent to the apex (Zonia et al., 2002). The spatial coupling of influx sites along the pollen tube and efflux site at the pollen tube apex predicts that as the apical Cl^- pool is depleted by cyclic efflux it can be refilled by the steady influx of Cl^- in adjacent regions (Fig. 7). These dynamics induce a vectorial flux of Cl^- anion traversing through the apical region of the pollen tube and promote a closed current surrounding the cell surface (Fig. 7).

Cl^- channel blockers inhibit pollen tube growth and induce rapid increases in the apical cell volume (Zonia et al., 2002). Hypoosmotic treatment that induces cell volume increases also induces an increased frequency of Cl^- efflux (Fig. 3). These data indicate that Cl^- flux correlates with the regulation of cell volume status in the pollen tube apical region. Information about the cell volume or intracellular hydrostatic pressure may be signaled to the Cl^- efflux oscillator by mechanosensitive ion channels located at the plasma membrane (Cosgrove and Hedrich, 1991). Activation of mechanosensitive channels by cell swelling or plasmolysis could also affect the membrane electrochemical potential. In this way mechanosensitive ion channels could rapidly input both positive and negative feedback signals to the Cl^- oscillator and thereby function as passive integrators regulating the cell volume status (Fig. 7).

Cl^- efflux is a mechanism used in both plant and vertebrate cells for regulating cell volume and hydrostatic pressure (Ward et al., 1995; Teodoro et al., 1998; Shabala et al., 2000; van der Wijk et al., 2000; Bali et al., 2001; Leonhardt et al., 2001; Okada et al., 2001; Roman et al., 2001; Wondergem et al., 2001), partly due to the capacity of anions to strongly affect the ordering and dynamics of water molecules in local domains (Kropman and Bakker, 2001; Kropman et al., 2002). Therefore, in addition to its correlation with cell volume regulation, Cl^- flux through the apical region of the pollen tube may have the potential to entrain a hydrodynamic flow that provides part of the driving force for cell elongation during growth (Zonia et al., 2002).

Previous work demonstrated that Ins(3,4,5,6)P_4 can act in regulatory circuits that inhibit pollen tube growth, induce cell volume increases, and disrupt Cl^- efflux (Zonia et al., 2002). The present report has demonstrated that Ins(3,4,5,6)P_4 inhibits the frequency of the Cl^- signal and induces transitions to period-tripling and higher-order multiplicative increases that may provide a route to chaos (Fig. 4). Thus, the combined evidence indicates that Ins(3,4,5,6)P_4 can act as a negative feedback regulator of Cl^- efflux oscillations (Fig. 7). Possible mechanisms for generating cyclic changes in the levels of Ins(3,4,5,6)P_4 could be via further phosphorylation/dephosphorylation cycles of Ins(1,4,5)P_3 to one of the immediate precursors Ins(3,4,6)P_3 or Ins(1,3,4,5,6)P_5 (Shears, 1996; Ho et al., 2000; Irvine and Schell, 2001).

The tip-localized cytosolic Ca^{2+} gradient and influx of extracellular Ca^{2+} through channels located at the pollen tube apex are necessary for pollen tube growth (Pierson et al., 1994, 1996; Holdaway-Clarke et al., 1997; Messerli et al., 1999, 2000). Both of these circuits oscillate with the same frequency as growth but are temporally out-of-phase with respect to the start of the growth cycle. There is evidence for a role for Ca^{2+} during cell swelling, in that a plasma membrane Ca^{2+} channel is rapidly activated by hypoosmotic stress in tobacco suspension cells and in *Fucus* and subsequently leads to increases in cytosolic Ca^{2+} (Takahashi et al., 1997; Taylor et al., 1997; Goddard et al., 2000). There is also evidence for the interaction of Ca^{2+} and Cl^-, in that anion channel activity in guard cells is stimulated by increases in cytosolic and extracellular Ca^{2+} (Schroeder and Hagiwara, 1989; Hedrich et al., 1990). In vertebrate secretory cells, the Cl^- efflux channel that is negatively regulated by Ins(3,4,5,6)P_4 is positively regulated by Ca^{2+} (Shears, 1996; Xie et al., 1998; Carew et al., 2000; Ho et al., 2001). Taken together, these results suggest the possibility that the nonlinear Ca^{2+} circuit that exists at the pollen tube apex may function at least in part as a positive feedback regulator of Cl^- efflux oscillations (Fig. 7).

The hypothesized reaction network shown in Fig. 7 containing three coupled nonlinear circuits (Cl^-, Ins(3,4,5,6)P_4, and Ca^2) meets the theoretical requirements for the generation of limit-cycle solutions (Tyson and Light, 1973; Murray, 1993) and may define a core signaling network that has the potential to entrain a basic motive force and coordinate the cellular events driving oscillatory pollen tube growth.

This work was supported by grants from the Czech Republic to L. Z. (Research Center Grant ''Signaling in Plants'' LN00A081MSMT; Grant Agency Fund (GACR, GA521/99/1354) and by a joint Czech-Portuguese Research Travel Grant. The vibrating probe was partially financed by Fundacao Luso-Americana para o Desenvolvimento (FLAD) to J. A. F.

REFERENCES

Acheson, D. 1997. From Calculus to Chaos: An Introduction To Dynamics. Oxford Univ. Press, Oxford. 269 pp.

Allen, G. J., S. P. Chu, C. L. Harrington, K. Schumacher, T. Hoffman, Y. Y. Tang, E. Grill, and J. I. Schroeder. 2001. A defined range of guard cell calcium oscillation parameters encodes stomatal movements. *Nature*. 411:1053–1057.

Allen, G. J., S. P. Chu, K. Schumacher, C. T. Shimazaki, D. Vafeados, A. Kemper, S. D. Hawke, G. Tallman, R. Y. Tsien, J. F. Harper, J. Chory, and J. I. Schroeder. 2000. Alteration of stimulus-specific guard cell calcium oscillations and stomatal closing in *Arabidopsis* det3 mutant. *Science*. 289:2338–2342.

Bali, M. Z., J. Lipecka, A. Edelman, and J. Fritsch. 2001. Regulation of ClC-2 chloride channels in T84 cells by TGF-alpha. *Am. J. Physiol. Cell Physiol.* 280:C1588–C1598.

Barrett, K. E., J. Smitham, A. Traynor-Kaplan, and J. M. Uribe. 1998. Inhibition of Ca^{2+}-dependent Cl^- secretion in T84 cells: membrane target(s) of inhibition is agonist specific. *Am. J. Physiol Cell Physiol.* 43:C958–C965.

Bohn, A., A. Geist, U. Rascher, and U. Lüttge. 2001. Responses to different external light rhythms by the circadian rhythm of crassulacean acid metabolism in *Kalanchoe daigremontiana*. *Plant Cell Environ*. 24:811–820.

Bohn, A., U. Rascher, M. T. Hutt, F. Kaiser, and U. Lüttge. 2002. Responses of a plant circadian rhythm to thermoperiodic perturbations with asymmetric temporal patterns and the rate of temperature change. *Biol. Rhythm Res.* 33:151–170.

Brearley, C. A., and D. E. Hanke. 1996. Inositol phosphates in the duckweed *Spirodela polyrhiza* L. *Biochem. J.* 314:215–225.

Brearley, C. A., and D. E. Hanke. 2000. Metabolic relations of inositol 3,4,5,6-tetrakisphosphate revealed by cell permeabilization. Identification of inositol 3,4,5,6-tetrakisphosphate 1-kinase and inositol 3,4,5,6-tetrakisphosphate phosphatase activities in mesophyll cells. *Plant Physiol.* 122:1209–1216.

Carew, M. A., X. N. Yang, C. Schultz, and S. B. Shears. 2000. myo-Inositol 3,4,5,6-tetrakisphosphate inhibits an apical calcium-activated chloride conductance in polarized monolayers of a cystic fibrosis cell line. *J. Biol. Chem.* 275:26906–26913.

Chen, Y., S. M. Simask, J. Niggel, W. J. Sigurdson, and F. Sachs. 1996. Ca^{2+} uptake in GH3 cells during hypotonic swelling: The sensory role of stretch-activated ion channels. *Am. J. Physiol.* 270:C1790–C1798.

Cosgrove, D. J., and R. Hedrich. 1991. Stretch-activated chloride, potassium, and calcium channels coexisting in plasma membranes of guard cells of *Vicia faba* L. *Planta*. 186:143–153.

Feijó, J. A., J. Sainhas, G. R. Hackett, J. G. Kunkel, and P. K. Hepler. 1999. Growing pollen tubes possess a constituitive alkaline band in the clear zone and a growth-dependent acidic tip. *J. Cell Biol.* 144:483–496.

Feijó, J. A., J. Sainhas, T. Holdaway-Clarke, S. Cordeiro, J. G. Kunkel, and P. K. Hepler. 2001. Cellular oscillations and the regulation of growth: the pollen tube paradigm. *Bioessays*. 23:86–94.

Goddard, H., N. F. H. Manison, D. Tomos, and C. Brownlee. 2000. Elemental propagation of calcium signals in response-specific patterns determined by environmental stimulus strength. *Proc. Natl. Acad. Sci. USA*. 97:1932–1937.

Hafke, J. B., R. Neff, M. T. Hutt, U. Lüttge, and G. Thiel. 2001. Day-to-night variations of cytoplasmic pH in a crassulacean acid metabolism plant. *Protoplasma*. 216:164–170.

Hedrich, R., H. Busch, and K. Raschke. 1990. Ca^{2+} and nucleotide dependent regulation of voltage dependent anion channels in the plasma membrane of guard cells. *EMBO J*. 9:3889–3892.

Hepler, P. K., L. Vidali, and A. Y. Cheung. 2001. Polarized cell growth in higher plants. *Annu. Rev. Cell Dev. Biol.* 17:159–187.

Higashiyama, T., H. Kuroiwa, S. Kawano, and T. Kuroiwa. 2000. Explosive discharge of pollen tube contents in *Torenia fournieri*. *Plant Physiol.* 122:11–13.

Ho, M. W. Y., M. A. Carew, X. Yang, and S. B. Shears. 2000. Regulation of chloride channel conductance by Ins(3,4,5,6)P_4; a phosphoinositide-initiated signaling pathway that acts downstream of Ins(1,4,5)P_3. *In* Biology of Phosphoinositides. S. Cockcroft, editor. Oxford University Press, Oxford. 298–319.

Ho, M. W. Y., M. A. Kaetzel, D. L. Armstrong, and S. B. Shears. 2001. Regulation of a human chloride channel. A paradigm for integrating input from calcium, type II calmodulin-dependent protein kinase, and inositol 3,4,5,6-tetrakisphosphate. *J. Biol. Chem.* 276:18673–18680.

Holdaway-Clarke, T., J. A. Feijó, G. R. Hackett, J. G. Kunkel, and P. K. Hepler. 1997. Pollen tube growth and the intracellular cytosolic calcium gradient oscillate in phase while extracellular calcium influx is delayed. *Plant Cell.* 9:1999–2010.

Irvine, R. F., and M. J. Schell. 2001. Back in the water: the return of the inositol phosphates. *Nat. Rev. Mol. Cell Biol.* 2:327–338.

Ismailov, I. I., C. M. Fuller, B. K. Berdiev, V. G. Shlyonsky, D. J. Benos, and K. E. Barrett. 1996. A biologic function for an ''orphan'' messenger: D-*myo*-inositol 3,4,5,6-tetrakisphosphate selectively blocks epithelial calcium-activated chloride channels. *Proc. Natl. Acad. Sci. USA*. 93:10505–10509.

Kropman, M. F., and H. J. Bakker. 2001. Dynamics of water molecules in aqueous solvation shells. *Science*. 291:2118–2120.

Kropman, M. F., H. K. Nienhuys, and H. J. Bakker. 2002. Real-time measurement of the orientational dynamics of aqueous solvation shells in bulk liquid water. *Phys. Rev. Lett.* 88:077601-1–077601-4.

Leonhardt, N., I. Bazin, P. Richaud, E. Marin, A. Vavasseur, and C. Forestier. 2001. Antibodies to the CFTR modulate the turgor pressure of guard cell protoplasts via slow anion channels. *FEBS Lett.* 494:15–18.

Lüttge, U. 2000. The tonoplast functioning as the master switch for circadian regulation of crassulacean acid metabolism. *Planta*. 211:761–769.

Mallat, S. 1999. A Wavelet Tour of Signal Processing, 2nd ed. Academic Press, San Diego and New York.

Mascarenhas, J. P. 1993. Molecular mechanisms of pollen tube growth and differentiation. *Plant Cell.* 5:1303–1314.

Messerli, M. A., R. Creton, L. F. Jaffe, and K. R. Robinson. 2000. Periodic increases in elongation rate precede increases in cytosolic Ca^{2+} during pollen tube growth. *Dev. Biol.* 222:84–98.

Messerli, M. A., G. Danuser, and K. R. Robinson. 1999. Pulsatile influxes of H^+, K^+ and Ca^{2+} lag growth pulses of *Lilium longiflorum* pollen tubes. *J. Cell Sci.* 112:1497–1509.

Messerli, M. A., and K. R. Robinson. 1998. Cytoplasmic acidification and current influx follow growth pulses of *Lilium longiflorum* pollen tubes. *Plant J.* 16:87–91.

Murray, J. D. 1993. Mathematical Biology, 2nd ed. Springer, Berlin and New York. 140–178.

Nilius, B., J. Prenen, T. Voets, J. Eggermont, K. S. Bruzik, S. B. Shears, and G. Droogmans. 1998. Inhibition by inositoltetrakisphosphates of calcium- and volume-activated Cl^- currents in macrovascular endothelial cells. *Pflugers Arch.* 435:637–644.

Okada, Y., E. Maeno, T. Shimizu, K. Dezaki, J. Wang, and S. Morishima. 2001. Receptor-mediated control of regulatory volume decrease (RVD) and apoptotic volume decrease (AVD). *J. Physiol. (Lond.)*. 532:3–16.

Oprins, J. C., C. van der Burg, H. P. Meijer, T. Munnik, and J. A. Groot. 2001. PLD pathway involved in carbachol-induced Cl^- secretion: possible role of TNF-α. *Am. J. Physiol. Cell Physiol.* 280:C789–C795.

Oprins, J. C., C. van der Burg, H. P. Meijer, T. Munnik, and J. A. Groot. 2002. Tumor necrosis factor alpha potentiates ion secretion induced by

histamine in a human intestinal epithelial cell line and in mouse colon: involvement of the phospholipase D pathway. *Gut*. 50:314–321.

Pierson, E. S., D. D. Miller, D. A. Callaham, A. M. Shipley, B. A. Rivers, M. Cresti, and P. K. Hepler. 1994. Pollen tube growth is coupled to the extracellular calcium ion and the intracellular calcium gradient: Effect of BAPTA-type buffers and hypertonic media. *Plant Cell.* 6:1815–1828.

Pierson, E. S., D. D. Miller, D. A. Callaham, J. Van Aken, G. Hackett, and P. K. Hepler. 1996. Tip-localized calcium entry fluctuates during pollen tube growth. *Dev. Biol.* 174:160–173.

Pittet, D., D. P. Lew, G. W. Mayr, A. Monod, and W. Schlegel. 1989. Chemoattractant receptor promotion of Ca^{2+} influx across the plasma membrane of HL-60 cells: a role for cytosolic free calcium elevations and inositol 1,3,4,5-tetrakisphosphate production. *J. Biol. Chem.* 264:7251–7261.

Rascher, U., B. Blasius, F. Beck, and U. Lüttge. 1998. Temperature profiles for the expression of endogenous rhythmicity and arrhythmicity of CO_2 exchange in the CAM plant *Kananchoe daigremontiana* can be shifted by slow temperature changes. *Planta*. 207:76–82.

Rascher, U., M. T. Hutt, K. Siebke, B. Osmond, F. Beck, and U. Lüttge. 2001. Spatiotemporal variation of metabolism in a plant circadian rhythm: The biological clock as an assembly of coupled individual oscillators. *Proc. Natl. Acad. Sci. USA*. 98:11801–11805.

Renstrom, E., R. Ivarsson, and S. B. Shears. 2002. Inositol 3,4,5,6-tetrakisphosphate inhibits insulin granule acidification and fusogenic potential. *J. Biol. Chem.* 277:26717–26720.

Roman, R. M., R. L. Smith, A. P. Feranchak, G. H. Clayton, R. B. Doctor, and J. G. Fitz. 2001. ClC-2 chloride channels contribute to HTC cell volume homeostasis. *Am. J. Physiol.-Gastro. Liver Physiol.* 280: G344–G353.

Schroeder, J. I., and S. Hagiwara. 1989. Cytosolic calcium regulates ion channels in the plasma membrane of *Vicia faba* guard cells. *Nature*. 338:427–430.

Shabala, S., O. Babourina, and I. Newman. 2000. Ion-specific mechanisms of osmoregulation in bean mesophyll cells. *J. Exp. Bot*. 51:1243–1253.

Shabala, S., R. Delbourgo, and I. Newman. 1997. Observations of bifurcation and chaos in plant physiological responses to light. *Aust. J. Plant Physiol.* 24:91–96.

Shears, S. B. 1996. Inositol pentakis- and hexakisphosphate metabolism adds versatility to the actions of inositol polyphosphates: novel effects on ion channels and protein traffic. *In* myo-Inositol Phosphates, Phosphoinositides, and Signal Transduction. Subcellular Biochemistry, Vol. 26. B. B. Biswas and S. Biswas, editors. Plenum Press, New York. 187–226.

Takahashi, K., M. Isobe, M. R. Knight, A. J. Trewavas, and S. Muto. 1997. Hypoosmotic shock induces increases in cytosolic Ca^{2+} in tobacco suspension culture cells. *Plant Physiol.* 113:587–594.

Taylor, L. P., and P. K. Hepler. 1997. Pollen germination and tube growth. *Annu. Rev. Plant Physiol. Plant Mol. Biol.* 48:461–491.

Taylor, A., N. Manison, and C. Brownlee. 1997. Regulation of channel activity underlying cell volume and polarity signals in *Fucus*. *J. Exp. Bot*. 48:579–588.

Teodoro, A. E., L. Zingarelli, and P. Lado. 1998. Early changes in Cl^- efflux and H^+ extrusion induced by osmotic stress in *Arabidopsis thaliana* cells. *Physiol. Plant*. 102:29–37.

Tyson, J. J., and J. C. Light. 1973. Properties of two-component bimolecular and trimolecular chemical reaction systems. *J. Chem. Phys.* 59:4164–4172.

Vajanaphanich, M., U. Kachintorn, K. E. Barrett, J. A. Cohn, K. Dharmsathaphorn, and A. Traynor-Kaplan. 1993. Phosphatidic acid modulates Cl^- secretion in T84 cells: vaying effects depending on mode of stimulation. *Am. J. Physiol. Cell Physiol.* 264:C1210–C1218.

Vajanaphanich, M., C. Schultz, M. T. Rudolf, M. Wasserman, P. Enyedi, A. Craxton, S. B. Shears, R. Y. Tsien, K. E. Barrett, and A. Traynor-Kaplan. 1994. Long-term uncoupling of chloride secretion from intracellular calcium levels by Ins(3,4,5,6)P_4. *Nature*. 371:711–714.

van der Wijk, T., S. F. B. Tomassen, H. R. de Jong, and B. C. Tilly. 2000. Signaling mechanisms involved in volume regulation of intestinal epithelial cells. *Cell. Physiol. Biochem*. 10:289–296.

Ward, J. M., Z.-M. Pei, and J. I. Schroeder. 1995. Roles of ion channels in initiation of signal transduction in higher plants. *Plant Cell*. 7:833–844.

Wondergem, N., W. Gong, S. H. Monen, S. N. Dooley, J. L. Gonce, T. D. Conner, M. Houser, T. W. Ecay, and K. E. Ferslew. 2001. Blocking swelling-activated chloride current inhibits mouse cell proliferation. *J. Physiol. (Lond.)*. 532:661–672.

Xie, W., K. R. H. Solomons, S. Freeman, M. A. Kaetzel, K. S. Bruzik, D. J. Nelson, and S. B. Shears. 1998. Regulation of Ca^{2+}-dependent Cl^- conductance in a human colonic epithelial cell line (T84): cross-talk between Ins(3,4,5,6)P_4 and protein phosphatases. *J. Physiol. (Lond.)*. 510:661–673.

Yang, X. N., M. Rudolf, R. A. Carew, M. Yoshida, V. Nerreter, A. M. Riley, S. K. Chung, K. S. Bruzik, B. V. L. Potter, C. Schultz, and S. B. Shears. 1999. Inositol 1,3,4-trisphosphate acts in vivo as a specific regulator of cellular signaling by inositol 3,4,5,6-tetrakisphosphate. *J. Biol. Chem.* 274:18973–18980.

Zonia, L., S. Cordeiro, and J. A. Feijó. 2001. Ion dynamics and the control of hydrodynamics in the regulation of pollen tube growth. *Sexual Plant Reprod.* 14:111–116.

Zonia, L., S. Cordeiro, J. Tupý, and J. A. Feijó. 2002. Oscillatory chloride efflux at the pollen tube apex has a role in growth and cell volume regulation and is targeted by inositol (3,4,5,6)-tetra*kis*phosphate. *Plant Cell.* 14:2233–2249.